

Physical basis of energy per cluster atom in the universal concept of sputtering

Robert J. Paruch, Zbigniew Postawa, and Barbara J. Garrison

Citation: *Journal of Vacuum Science & Technology B* **34**, 03H105 (2016); doi: 10.1116/1.4940153

View online: <http://dx.doi.org/10.1116/1.4940153>

View Table of Contents: <http://scitation.aip.org/content/avs/journal/jvstb/34/3?ver=pdfcov>

Published by the AVS: Science & Technology of Materials, Interfaces, and Processing

Articles you may be interested in

[Second order classical perturbation theory for the sticking probability of heavy atoms scattered on surfaces](#)

J. Chem. Phys. **143**, 064706 (2015); 10.1063/1.4928432

[Hyperthermal Ar atom scattering from a C\(0001\) surface](#)

J. Chem. Phys. **128**, 224708 (2008); 10.1063/1.2924126

[High-energy ions and atoms sputtered and reflected from a magnetron source for deposition of magnetic thin films](#)

J. Vac. Sci. Technol. A **23**, 671 (2005); 10.1116/1.1943452

[Packing density and structure effects on energy-transfer dynamics in argon collisions with organic monolayers](#)


J. Chem. Phys. **122**, 234714 (2005); 10.1063/1.1924693

[Self-sputtering of silver by mono- and polyatomic projectiles: A molecular dynamics investigation](#)

J. Chem. Phys. **115**, 8643 (2001); 10.1063/1.1404982

HIDEN
ANALYTICAL

Instruments for Advanced Science

 <p>Gas Analysis</p> <ul style="list-style-type: none">dynamic measurement of reaction gas streamscatalysis and thermal analysismolecular beam studiesdissolved species probesfermentation, environmental and ecological studies	 <p>Surface Science</p> <ul style="list-style-type: none">UHV TPDSIMSend point detection in ion beam etchelemental imaging - surface mapping	 <p>Plasma Diagnostics</p> <ul style="list-style-type: none">plasma source characterizationetch and deposition process reactionkinetic studiesanalysis of neutral and radical species	 <p>Vacuum Analysis</p> <ul style="list-style-type: none">partial pressure measurement and control of process gasesreactive sputter process controlvacuum diagnosticsvacuum coating process monitoring
--	---	---	---

Contact Hiden Analytical for further details:
W www.HidenAnalytical.com
E info@hiden.co.uk
CLICK TO VIEW our product catalogue

Physical basis of energy per cluster atom in the universal concept of sputtering

Robert J. Paruch^{a)}

Department of Chemistry, Penn State University, 104 Chemistry Building, University Park, Pennsylvania 16802

Zbigniew Postawa

Smoluchowski Institute of Physics, Jagiellonian University, ulica Lojasiewicza 11, 30-348 Krakow, Poland

Barbara J. Garrison

Department of Chemistry, Penn State University, 104 Chemistry Building, University Park, Pennsylvania 16802

(Received 13 November 2015; accepted 7 January 2016; published 19 January 2016)

The interpretation of the variables, scaled by the number of projectile cluster atoms n , in the universal relation of the sputtering yield Y versus incident energy E , that is, Y/n vs E/n , is not necessarily obvious. Following on previous works, the objective of this study is to elucidate the physical basis of the energy per atom variable E/n . The authors employ molecular dynamics simulations of Ar_n cluster bombardment of $\text{Ag}(111)$ metal samples for this study. The authors find that the energy per cluster atom quantity E/n is responsible for the fraction of the initial energy that is deposited in the solid, rather than energy per cluster mass E/m . The results show that even though there is an average loss of the energy for a cluster, each cluster atom loses a different fraction of its initial energy, thus yielding a distribution of energy loss by individual atoms. The analysis of these distributions indicates that the energy deposition process is more effective for clusters with higher E/n when compared to the clusters with lower E/n . This conclusion is supported by a visual analysis of the cluster bombardment event. The cluster atoms that lose most of their initial energy are those which split off from the cluster and penetrate into the bulk of the solid. Conversely, the atoms of the clusters with low E/n keep together during the interaction with the solid, and eventually reflect into the vacuum taking away a portion of the initial kinetic energy. In addition, the simulations indicate that the clusters of different sizes have the same distribution of energy loss for individual atoms if they have the same E/n , in other words, if the initial energy E is proportional to the cluster size n . © 2016 American Vacuum Society.

[<http://dx.doi.org/10.1116/1.4940153>]

I. INTRODUCTION

Experimental applications of energetic cluster beams include surface fabrication, surface modification, and the analytical technique of secondary-ion mass spectrometry (SIMS).^{1,2} Gas cluster projectiles, which appear to cause minimal damage to the organic substrate, have turned out to be useful in depth profiling and three-dimensional imaging of organic materials, with high depth resolution and chemical specificity.^{3,4} Theoretical studies were undertaken, including computer modeling by molecular dynamics (MD) simulations, in order to understand the basic processes and to help optimize experimental conditions.⁵ During these studies, an interesting observation was made that the scatter in data points in the dependence of the sputtering yield Y against the incident kinetic cluster energy E for different clusters sizes can be reduced to nearly a curve, if the variables Y and E are presented in quantities scaled by the number of cluster atoms n , that is, Y/n vs E/n .⁶ This observation was then confirmed by numerous studies, both experimental^{7,8} and computational,^{9–11} for various solids (Ag , Si , SiO_2 ,

Irganox , and polystyrene) and the cluster beams (C_{60} , Ar_n). The results for atomic and molecular solids, however, separate into two distinct regions on a Y/n vs E/n plot.⁸ The observed feature suggests that a universal description of the cluster sputtering process might be possible if appropriate scaling of the variables is used, although the physical basis of this phenomenon was not clear.

In our previous works, we investigated the concept of universality in sputtering yields based on results of MD simulations. The model samples of $\text{Ag}(111)$ and molecular solids (benzene, octane, and β -carotene) were sputtered by Ar_n clusters.^{12–14} We demonstrated that a better representation to improve the convergence between the data points for atomic and molecular solids is $Y/(E/U_0)$ vs $(E/U_0)/n$, where U_0 is the binding energy of the solid. U_0 is defined per atom and per molecule for atomic and molecular solids, respectively. Consequently, the yield Y is given in atoms and molecules for atomic and molecular solids, respectively. As explained previously in greater detail, to arrive at this form of the scaled representation, we replaced n by E in the Y/n variable, and, following others,^{6,15,16} scaled E by U_0 . The first change was justified by the fact that for a given E/n value, the cluster size n relates proportionately to the cluster energy E .^{12,13}

^{a)}Electronic mail: rjp25@psu.edu

This change is the basis of the physical interpretation of the variable Y/n as explained below. The second change was needed in order to take into account the fact that the binding energies U_0 , for atomic and molecular solids, can differ several times; thus, their effect on the sputtering efficiency cannot be neglected.^{14,17} The results of MD simulations showed that there are obvious similarities in the sputtering mechanisms between the atomic and molecular solids for almost 3 orders of magnitude variation of $(E/U_0)/n$, therefore supporting the statement of universality.¹⁴ The conclusion from the analysis of the universal relation with regard to the physical meaning of the ordinate variable Y/n is that, for a given E/n value, the dependence of the sputtering yield Y on the cluster size n is equivalent to the dependence of Y on the incident cluster energy E . This interpretation makes more physical sense because the cluster energy E is the primary factor inducing ejection rather than the cluster size n .

The aim of this paper is to address the question of the physical meaning of the abscissa variable in the universal relation. The abscissa variable has generally been interpreted as the incident energy per cluster atom E/n .^{6,12,13,17} It has also been interpreted as a quantity proportional to the squared velocity of the cluster, and as such presented as the energy per cluster mass E/m if results for different cluster types were compared on the same plot.^{9–11} It is not intuitively obvious which variation, E/n or E/m , is correct, although the “velocity” interpretation fits with the bead model that considers the whole cluster as a single particle losing energy due to friction.^{18,19} For this study, we analyzed MD simulations of a model system, in which Ag(111) samples were bombarded by Ar_n clusters. Ar_n clusters are currently popular beam sources for organic SIMS, whereas Ag(111) is a convenient metal substrate for MD modeling of SIMS experiments. As explained above, scaling of E by U_0 is needed in the universal description if results for sputtering of different solids are being compared. Since in this study we use only one sample, we omit the scaling by U_0 for simplicity. The binding energy of the Ag sample calculated from the interaction potential used in the simulations is 2.95 eV per atom.

II. COMPUTATIONAL

The setup of the MD simulations was described in greater detail previously.^{12,20,21} Rectangular boxes of Ag(111) samples, measuring approximately from $26 \times 26 \times 13$ to $31 \times 31 \times 23$ nm and containing approximately from 600 000 to 1 400 000 Ag atoms, were used depending on the projectile cluster size and impact energy. The interactions between the cluster atoms, Ar–Ar, and between the cluster atoms and the substrate atoms, Ar–Ag, were described by the Lennard–Jones potential splined with the KrC potential to account properly for high-energy collisions.²² The MD/Monte Carlo corrected effective medium potential was used for the interactions in the metal substrate, Ag–Ag.²³ In order to ease identification of the most characteristic features of the bombardment event, a simple geometry was used, that is, a flat (111) crystal face was irradiated at normal incidence.

To improve the statistical relevance of the findings, the analysis was based on MD trajectories that have sputtering yields close to the average values for given beam conditions.²⁰ The calculations were performed at 0 K.

III. RESULTS AND DISCUSSION

A. Effect of changing the cluster energy E at given cluster size n

First, we examine the dynamics of the energy deposition process for clusters of the same size n and various initial kinetic energies E , that is, for variable kinetic energy per cluster atom E/n . Figure 1(a) compares energy loss in time for Ar_{366} impinging an Ag(111) substrate at three different values of E/n . The ordinate is the fraction of the energy that the cluster retains. It appears that the Ar_{366} cluster deposits a different fraction of initial kinetic energy depending on the value of E/n . Low E/n clusters retain more energy, thus giving less energy to the substrate than high E/n clusters. We identified two characteristic points in time of the energy deposition event. Previous studies showed that the initial energy loss of the cluster follows that of friction on a single particle or bead until the cluster deposits approximately 60% of the energy that is finally deposited.^{18,19} The point when 60% of the final deposited energy has been deposited is marked on each of the energy loss curves in Fig. 1 with a circle marker. This point will be referred to as the bead configuration. The second point is chosen to represent the configuration when most of the cluster deceleration in the solid has occurred. We assume that it corresponds to the moment when 90% of the final deposited energy has been deposited. As demonstrated previously,^{16,24} this amount of deposited energy is responsible for ejection of a considerable portion of material. This point is marked in each of the energy loss curves in Fig. 1 with a square marker and will be referred to as the stopping configuration. Of note is that the final retained energy, that is, the energy that is not deposited in the solid, goes into the kinetic energy of the reflected cluster atoms.

Figure 2 shows snapshots from simulations of Ar_{366} cluster impinging an Ag(111) substrate taken at the times marked on the curves in Fig. 1(a). Figures 2(a)–2(c) show snapshots of the bead configuration for Ar_{366} with the three different values of E/n . It appears that the atoms of the cluster are more or less together albeit the cluster is deformed. At the highest E/n , Ar atoms have started to split off from the cluster and penetrated into the solid. At the lowest E/n , the cluster has for the most part only flattened. The penetration depth of the bulk of the cluster in the solid is in all three cases similar, approximately 1 nm. We conclude that up to this moment of the energy deposition process, the physics of energy loss follows that of friction on a single particle and the clusters behave like a single bead experiencing frictional forces.^{18,19} Figures 2(d)–2(f) show snapshots of the stopping configuration for Ar_{366} with the three different values of E/n . At the highest E/n , the cluster has broken up. Due to high energy per cluster atom, individual cluster atoms penetrate into the bulk of the solid.¹⁴ The penetration depth exceeds 2 nm. At the lowest E/n , the picture does not change much.

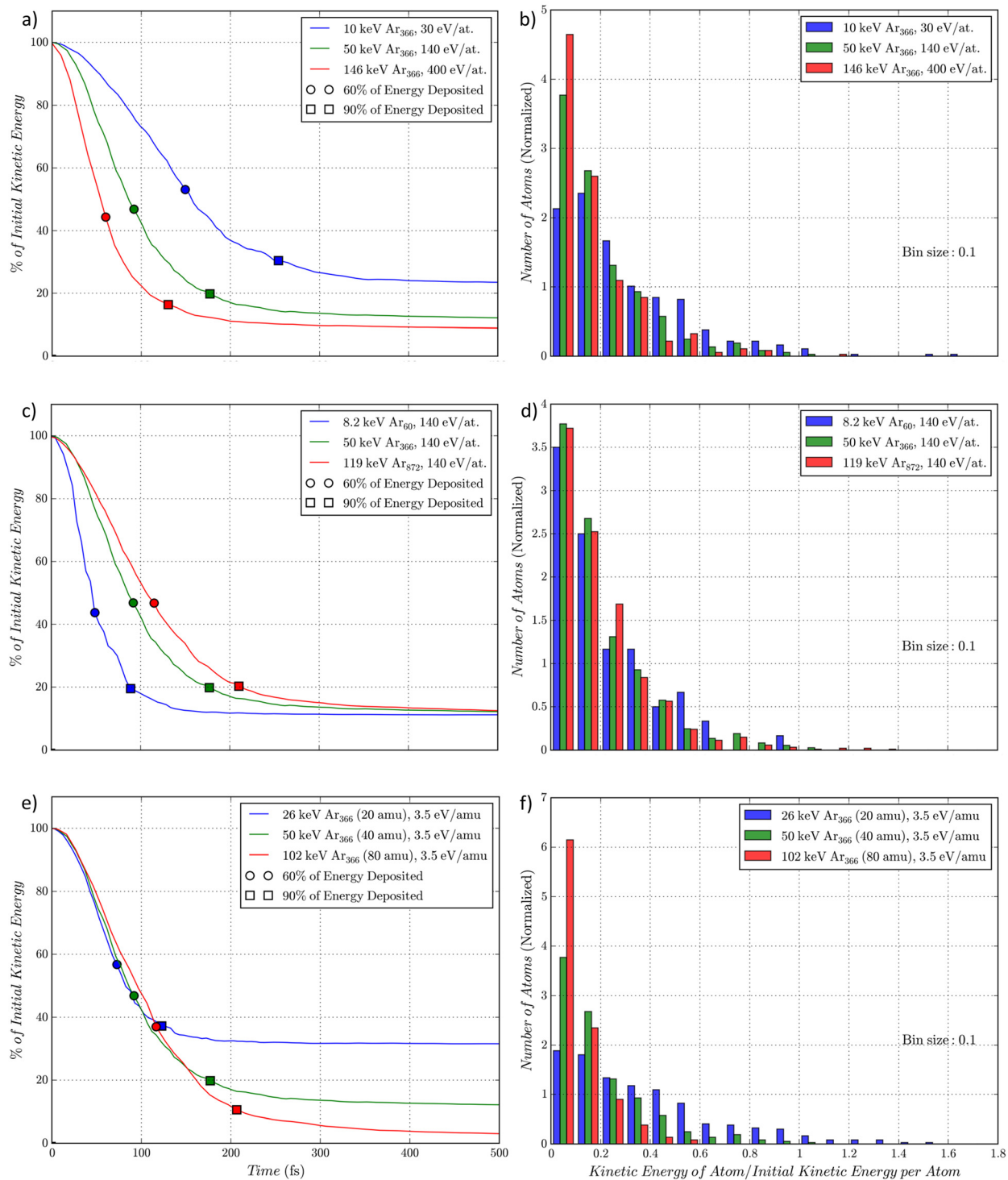


Fig. 1. (Color online) [(a), (c), and (e)] Fraction of initial kinetic energy E retained by the cluster vs time. The substrate is Ag(111). The times for the bead configuration (60% of energy deposited) and stopping configuration (90% of energy deposited) are marked on the energy loss curves. [(b), (d), and (f)] Histogram of the number of cluster atoms that have a given fraction of their initial kinetic energy at the stopping configuration. The bin size for the histogram is 0.1. The presented results are for the following beam conditions: [(a) and (b)] Ar_{366} cluster for three values of incident energy per cluster atom $E/n = 30, 140$, and 400 eV/atom. [(c) and (d)] Ar_{60} , Ar_{366} , and Ar_{872} clusters for $E/n = 140$ eV/atom. [(e) and (f)] Ar_{366} cluster for three masses of the cluster atoms, 20, 40, and 80 amu, at three values of $E/n = 70, 130$, and 270 eV/atom, respectively, or a common value of incident energy per cluster mass $E/m = 3.5$ eV/amu.

The cluster atoms keep together within the basin of deformed surface¹⁴ and the penetration depth remains approximately 1 nm. The energy per cluster atom is not sufficient for the cluster atoms to penetrate into the solid. At the middle E/n , there is an intermediate configuration, with the

penetration depth exceeding 1 nm. It is clear from the snapshots in Fig. 2 that the energy is deposited before virtually any ejection of the substrate atoms has occurred.^{16,25} At this point, the disruption of the substrate is confined to the area directly affected by the cluster. Of note is that, although the

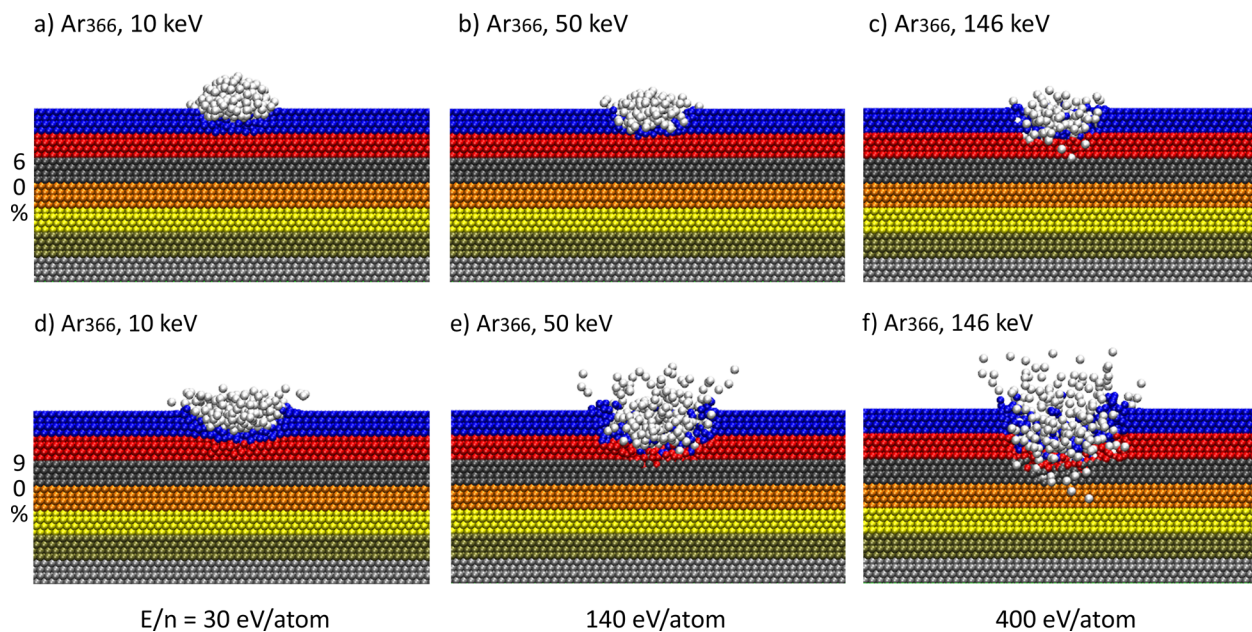


FIG. 2. (Color online) Snapshots of Ar_{366} cluster (white) and substrate $\text{Ag}(111)$ interaction for three values of incident energy per projectile atom $E/n = 30$, 140, and 400 eV/atom. Shown is a slice of the sample, 1.5 nm thick and centered at the point of the cluster impact. The marked sample layers correspond to four atomic layers with a thickness of approximately 1 nm each. The times for the bead and stopping configurations are shown in Fig. 1(a). [(a)–(c)] The cluster at bead configuration. [(d)–(f)] The cluster at stopping configuration.

penetration depth during the energy deposition process depends on E/n , eventually almost all the cluster atoms (99%) depart from the solid. The cluster atoms are either reflected from the surface in the initial phase of the bombardment event or are ejected together with the substrate atoms in subsequent stages.

Figure 1(b) shows the distribution of the number of cluster atoms that have a given fraction of their initial kinetic energy at the stopping configuration, for the three cases discussed above. First, even though there is an average energy loss per atom, as shown in Fig. 1(a), not every atom loses the same amount of its initial energy. The distribution for the highest E/n value (red) peaks at the lowest values of abscissa and the tail of the distribution is shorter compared to the other distributions. It indicates that most of the atoms lose a considerable fraction of their initial energy. The transfer of energy to the solid is the most efficient. Conversely, for the lower E/n values (green and blue), the centers of the distributions are shifted toward higher values of abscissa. In these cases, the cluster atoms retain more of the initial energy, and, eventually, more energy is reflected from the surface into the vacuum. The distributions correlate with the snapshots shown in Figs. 2(d)–2(f). The Ar atoms that have split off from the cluster are losing the most energy. Those that do not break off cannot lose as much of their initial energy.

The trend observed in Fig. 1(a) can now be explained as follows. The cluster with the highest E/n deposits the highest fraction of its initial energy because the energy deposition process is the most efficient. It is a result of the cluster atoms having sufficiently high energy for some of the atoms to penetrate into the solid. For the clusters with lower E/n , the transfer of the energy occurs only at the

deformed surface of the sample. As the result, the cluster atoms retain more energy, which is then reflected from the surface.

B. Effect of changing the cluster size n at given E/n

The energy loss of the cluster as a function of time is shown in Fig. 1(c) for three Ar clusters of size 60, 366, and 872 atoms, all at $E/n = 140$ eV/atom. It is apparent that the clusters eventually lose the same fraction of their initial energy, independent of the cluster size. The corresponding distributions of the energies of the cluster atoms at the stopping configuration are shown in Fig. 1(d). The distributions are similar for the three cluster sizes. It appears that regardless of the cluster size, the distributions of the final energies of the cluster atoms are essentially the same (have the same average values) if clusters of different sizes have the same E/n , that is, the initial kinetic energy E is proportional to the cluster size n . Such clusters deposit in the solid equal fractions of their initial energies, as shown in Fig. 1(c).

C. Effect of changing the cluster mass m at given E/m

The comparison made so far has been for clusters of one atom type. The challenges arise when one is comparing the sputtering yields that result from the bombardment of different cluster types, such as C_n , Ar_n , and Bi_n . We will not belabor this issue as it is fraught with difficulties, but we will comment on the use of E/n vs E/m because it can be easily tested. It has been proposed that the initial velocity of the cluster be the critical quantity for the description of the energetic cluster interaction with a solid.²⁶ This suggestion justified the use of E/m since this quantity is proportional to the

velocity squared for different cluster types. For the test cluster, we used Ar₃₆₆ with artificial masses of 20, 80, 107, and 150 amu. The results for the latter two are not shown here as they overlap those for 80 amu. The energy loss of the cluster as a function of time is shown in Fig. 1(e). The clusters composed of heavier atoms lose on average more energy than the lighter clusters. Since the cluster with 80 amu atoms deposits nearly all of its initial energy, so do the clusters with 107 and 150 amu atoms. The light Ne-like atoms (20 amu) mostly reflect from the surface into vacuum taking away large fraction of their initial energy, as shown in Fig. 1(f), where the distribution for 20 amu (blue) has the center shifted toward higher values of abscissa when compared to the other two. Conversely, the heavier atoms penetrate more deeply and lose more of their initial energy to the substrate as apparent in Fig. 1(f), where the distribution for 80 amu (red) peaks at lower values of the abscissa. This observation indicates that different cluster types, which have the same size and initial velocity, that is, the value of E/m , lose different fraction of their initial kinetic energy. Therefore, comparing different cluster types on E/m basis is not appropriate.

IV. SUMMARY AND CONCLUSIONS

Based on the results of MD simulations of Ar_n cluster bombardment of Ag(111) metal substrate, we found that the fraction of the initial energy deposited by a cluster in the solid depends on the quantity E/n . The clusters with higher energy per atom E/n lose a larger fraction of the initial energy when compared to the cluster with lower E/n . Even though there is an average loss of the energy for a cluster, each cluster atom loses a different fraction of its initial energy. The analysis of the distributions of the final energies of the cluster atoms indicates that the energy deposition process is the most effective for atoms with higher energy per atom. This observation is supported by a visual evaluation of the cluster bombardment event. The cluster atoms that lose most of the initial energy are those which split off from the cluster and penetrate into the bulk of the solid. Conversely, the atoms of the clusters with low E/n keep together during the interaction with the solid, and eventually reflect into the vacuum taking away a portion of their initial energy. The results show that the clusters of different sizes lose the same fraction of the initial energy if they have the same E/n , in other words, if the initial energy E is proportional to the cluster size n . Regardless of the cluster size, the distributions of the final cluster atom energies are similar. The results also show that different type clusters deposit a different fraction of the initial energy event though they have the same value of E/m , a quantity which is related to cluster velocity squared for clusters of different types. Therefore, comparing the

sputtering yields that result from the bombardment of different cluster types on the E/m basis is not appropriate.

ACKNOWLEDGMENTS

The authors gratefully acknowledge the financial support from the National Science Foundation, Grant No. CHE-1212645, and the Polish National Science Center, Grant No. 2013/09/B/ST4/00094. The authors appreciate the support of the Penn State Institute for CyberScience in performing these simulations. The visualization of data presented in this paper was done with the matplotlib Python library²⁷ and the Visual Molecular Dynamics Program.²⁸

¹N. Winograd, *Anal. Chem.* **77**, 142A (2005).

²N. Winograd and B. J. Garrison, *Annu. Rev. Phys. Chem.* **61**, 305 (2010).

³I. Yamada, J. Matsuo, N. Toyoda, and A. Kirkpatrick, *Mater. Sci. Eng., R* **34**, 231 (2001).

⁴A. G. Shard *et al.*, *Anal. Chem.* **84**, 7865 (2012).

⁵B. J. Garrison and Z. Postawa, *ToF-SIMS: Surface Analysis by Mass Spectrometry*, edited by J. C. Vickerman and D. Briggs (IM/SurfaceSpectra, Manchester, 2013).

⁶C. Anders, H. M. Urbassek, and R. E. Johnson, *Phys. Rev. B* **70**, 155404 (2004).

⁷L. Yang, M. P. Seah, and I. S. Gilmore, *J. Phys. Chem. C* **116**, 23735 (2012).

⁸M. P. Seah, *Surf. Interface Anal.* **47**, 169 (2015).

⁹A. Delcorte, B. J. Garrison, and K. Hamraoui, *Anal. Chem.* **81**, 6676 (2009).

¹⁰G. Palka, L. Rzeznik, R. Paruch, and Z. Postawa, *Acta Phys. Pol., A* **123**, 831 (2013).

¹¹A. Delcorte, V. Cristaudo, V. Lebec, and B. Czerwinski, *Int. J. Mass Spectrom.* **370**, 29 (2014).

¹²R. J. Paruch, B. J. Garrison, M. Mlynek, and Z. Postawa, *J. Phys. Chem. Lett.* **5**, 3227 (2014).

¹³R. J. Paruch, B. J. Garrison, M. Mlynek, and Z. Postawa, *J. Phys. Chem. Lett.* **5**, 3435 (2014).

¹⁴R. J. Paruch, Z. Postawa, and B. J. Garrison, *Acc. Chem. Res.* **48**, 2529 (2015).

¹⁵C. Anders and H. M. Urbassek, *Nucl. Instrum. Methods Phys. Res., Sect. B* **228**, 84 (2005).

¹⁶M. F. Russo and B. J. Garrison, *Anal. Chem.* **78**, 7206 (2006).

¹⁷M. P. Seah, *J. Phys. Chem. C* **117**, 12622 (2013).

¹⁸B. J. Garrison, K. E. Ryan, M. F. J. Russo, E. J. Smiley, and Z. Postawa, *J. Phys. Chem. C* **111**, 10135 (2007).

¹⁹K. E. Ryan, M. F. Russo, Jr., E. J. Smiley, Z. Postawa, and B. J. Garrison, *Appl. Surf. Sci.* **255**, 893 (2008).

²⁰L. Rzeznik, R. Paruch, B. J. Garrison, and Z. Postawa, *Nucl. Instrum. Methods Phys. Res., Sect. B* **269**, 1586 (2011).

²¹R. J. Paruch, Z. Postawa, and B. J. Garrison, *Surf. Interface Anal.* **46**, 253 (2014).

²²R. A. Aziz and M. J. Slaman, *Mol. Phys.* **58**, 679 (1986).

²³C. L. Kelchner, D. M. Halstead, L. S. Perkins, N. M. Wallace, and A. E. DePristo, *Surf. Sci.* **310**, 425 (1994).

²⁴M. F. Russo, Jr., K. E. Ryan, B. Czerwinski, E. J. Smiley, Z. Postawa, and B. J. Garrison, *Appl. Surf. Sci.* **255**, 897 (2008).

²⁵M. F. Russo, C. Szakal, J. Kozole, N. Winograd, and B. J. Garrison, *Anal. Chem.* **79**, 4493 (2007).

²⁶A. Delcorte and B. J. Garrison, *J. Phys. Chem. C* **111**, 15312 (2007).

²⁷J. D. Hunter, *Comput. Sci. Eng.* **9**, 90 (2007).

²⁸W. Humphrey, A. Dalke, and K. Schulten, *J. Mol. Graphics* **14**, 33 (1996).